tectable mechanical or morphological alterations. The equilibrium sorption isotherm for both the control and lipid extracted epidermis is shown in Figure 5. The selective removal of the lipid components of the epidermis appears to have no effect on the equilibrium sorption characteristics of the skin. Furthermore, the sorption isotherm can be similarly split into the dissolved and immobilized components as shown in Figure 5. In this case, the values of the constants K_D, C_I^*, and b are, respectively, 1.1, 36.0 mg/ml and 0.11 ml/mg.

The average steady state diffusion coefficients determined by dividing the measured steady state flux by the computed gradient of dissolved drug are shown in Table 2. Lipid extraction of the skin prior to permeation measurements results in a 500 fold increase in the steady state diffusivity. Similarly, a comparison is made between the ratio of the steady state to time lag diffusion coefficients measured experimentally as a function of concentration, and the ratio predicted by using Equation (11), and is shown in Figure 6. Again, the agreement between theory and experiment is good.

CONCLUSIONS

We have been able to demonstrate the basic validity of the dual mode sorption model and its usefulness in the analysis of the permeation characteristics of scopolamine through human skin in vitro. The interstitial lipid phase of the stratum corneum is the cause for the exceedingly low apparent diffusivity of scopolamine and in this regard acts as the principal permeation barrier. Selective removal of the lipid phase of the stratum corneum enhances the transdermal permeation rate of scopolamine by orders of magnitude without causing any change in the equilibrium sorption isotherm, suggesting that scopolamine sorbed by the skin is localized predominantly within the protein phase of the tissue.

NOTATION

a = b/K_D = constant
b = Langmuir's isotherm constant
C = concentration
C_D = mobile concentration
C_I = immobilized concentration
C_I^* = Langmuir's isotherm constant
C_T = total concentration
D = diffusion coefficient
D_{SS} = steady state diffusion coefficient
D_{TL} = time lag diffusion coefficient
J = flux
K_D = partition coefficient
l = membrane thickness
t = time
x = distance
θ = diffusion time lag

LITERATURE CITED

Anderson, R. L., and J. M. Cassidy, "Variations in Physical Dimensions and Chemical Composition of Human Stratum Corneum," *J. Invest. Dermatol.*, **61**, 30 (1973).

Assink, R. A., "Investigation of the Dual Mode Sorption of Ammonia in Polystyrene by NMR," *J. Polymer Sci.*, **13**, 1665 (1975).

Frisch, H. L., "The Time Lag in Diffusion," *J. Phys. Chem.*, **61**, 93 (1957).

Katz, M., and B. J. Poulsen, "Absorption of Drugs through the Skin," in *Handbuck der Experimentellen Pharmacologie; Concepts in Biochemical Pharmacology, Part 1*, B. B. Brodie and J. R. Gillett, ed., Springer Verlag, New York (1971).

Michaels, A. S., S. K. Chandrasekaran, and J. E. Shaw, "Drug Permeation through Human Skin: Theory and *In Vitro* Experimental Measurement," *AIChE J.*, **21**, 985 (1975).

Michaels, A. S., W. R. Vieth, and J. A. Barrie, "Solution of Gases in Polyethylene Terephthalate," *J. Appl. Phys.*, **34**, 1 (1963).

Paul, D. R., "Effect of Immobilizing Adsorption on the Diffusion Time Lag," *J. Polymer Sci.*, **7**, 1811 (1969).

———, and D. R. Kemp, "The Diffusion Time Lag in Polymer Membranes Containing Adsorptive Fillers," *ibid.*, **41**, 79 (1973).

Scheuplein, R. J., and I. H. Blank, "Permeability of the Skin," *Physiol. Rev.*, **51**, 702 (1971).

Manuscript received March 29, 1976; revision received May 25, and accepted May 26, 1976.

Shear Viscosity of Native and Enzyme Hydrolyzed Amioca Starch Pastes

Shear viscosity of an Amioca starch paste undergoing hydrolysis by immobilized α-amylase is shown to follow a power law behavior. The power law constants are uniquely related in a way which reduces the power law to a dimensionless form, a result previously reported only for retrograding starch and coagulating milk. The concept of a total hydrodynamic volume [Amioca starch molecules (amylopectin) plus associated immobilized liquid] is extended to concentrations above the dilute solution regime. A molecular interpretation is proposed for the shear viscosity behavior of Amioca starch pastes vs. extent of starch hydrolysis.

ANGEL CRUZ
WILLIAM B. RUSSEL
and
DAVID F. OLLIS
Chemical Engineering Department
Princeton University
Princeton, New Jersey 08540

SCOPE

For viscous media such as those commonly encountered in the food, textile, and paper industries, useful immobilized enzyme catalyst configurations are notably lacking. This paper presents a novel, monolithic enzyme mesh, supported on a rotating or reciprocating agitator, which is shown to be active in moderately viscous media (1 to 5 poise).

The pseudoplastic fluids examined are 1.0 to 4.7% wt/

vol pastes of cooked Amioca (waxy maize) starch granules. The hydrolysis and shear viscosity behavior of these pastes is reported for varying extents of hydrolysis by the enzyme paddle catalyst. [Enzyme-paddle preparation and hydrolytic activity in low viscosity solutions of high molecular weight polysaccharides are shown elsewhere (Cruz and Ollis, 1976).]

Shear stress vs. shear rate curves are employed in this paper to monitor the progress of enzyme degradation of the medium. The shear viscosity magnitude and shear rate dependence are found to be quite sensitive to the extent of paste hydrolysis. From these results, a convenient parameter for monitoring the extent of enzyme catalyzed modifications of viscous media is suggested.

CONCLUSIONS AND SIGNIFICANCE

The power law, $\tau = K\gamma^N$, can describe the shear viscosity of native or partially hydrolyzed Amioca starch paste from 0.63 to 4.8% wt/vol concentrations for temperatures between 23° to 60°C and shear rates in the range 3.0 to 230 s^{-1}.

For partially hydrolyzed starch pastes, a unique relationship between the two power law constants K,N is found similar to results for retrograding starch (Nedonchelle and Schutz, 1967) and coagulating milk (Tusznski and Scott Blair, 1967). This relation implies that all native or partially hydrolyzed samples of a given starch concentration behave indistinguishably at a common shear stress and shear rate (τ_o, γ_o). This common intersection obtained by extrapolation of log τ vs. log γ data can be considered as the high shear limiting viscosity ($\eta^\infty = \tau_o/\gamma_o$) at which all starch structure has been reduced to the same effective suspension by shear and/or hydrolysis.

The total hydrodynamic volume ϕ_e, including polymer plus immobilized liquid, is shown to provide a useful correlating parameter for Amioca (branched) starch paste similar to that found for linear polymers (Dreval et al., 1973; Simha and Utracki, 1973). The viscosity-volume fraction relationship defined by ϕ_e resembles that for rigid spheres in the dilute regime and approaches that of a fluid containing deformable particulates (emulsions and suspensions of blood cells) at higher concentrations. Because of the linear log (η_r) vs. ϕ_e relationship at higher ϕ_e values, shear viscosities can be easily related to values of ϕ_e, thereby allowing viscometric monitoring of starch paste enzymatic hydrolysis. This result could prove useful in both process control and process testing applications.

Starch pastes and their moderately concentrated solutions (~2% wt/vol) exhibit shear viscosity behavior dependent upon the starch origin, concentration, and method of preparation. Subsequent enzyme hydrolysis alters the non-Newtonian behavior of the starch pastes in ways which may be influenced by the enzyme specificity for terminal vs. internal bond hydrolysis. These factors are among those responsible for the inadequate rheological characterization of cooked or partially hydrolyzed starch pastes.

Starch granules from most plant species contain two types of polysaccharides. The starch paste shear thinning behavior under steady state or transient conditions (pseudoplasticity and thixotropy, respectively) depends on the relative proportions of these two constituents. The major component, amylopectin, comprises 70 to 80% of most starches and posesses a branched bushlike structure with linear chain segments averaging 20 to 25 α-(1 → 4) linked glucose residues between branching α-(1 → 6) linkages. Amylose, the minor component, is a linear unbranched glucose polymer (Williams, 1968). Some starch granules such as those of waxy maize contain as little as 1% amylose (Powell, 1973). Pure amylose solutions are thixotropic, while those of only amylopectin are pseudoplastic within the response times of typical viscometers (Storey and Merrill, 1958).

Correlations for the shear dependent viscosity of pseudoplastic materials are generally derived by considering competing rate processes. Molecular entanglements, contact points, or association links are assumed to exist between the primary particles (for example, molecules). Expressions for rates of formation and rupture of these links including Brownian motion and shear influences are formulated (Storey and Merrill, 1958; Gillespie, 1966; Cross, 1969). All such models for shear viscosity η vs. shear rate γ have the form

$$\eta = C_1 + \frac{C_2}{1 + C_3\gamma^n} \qquad (1)$$

The interpretation of the material constants n, C_1, C_2, and C_3 varies from model to model.

These models all suffer similar drawbacks. Accurate evaluation of constants requires viscosity measurements over a wide range of shear rates γ. In this study, the shear rate range was limited to the range $1.0 \leq \gamma \leq 230$ s^{-1}. Consequently, extensive extrapolations were necessary to estimate the model parameters. The resulting errors rendered futile the interpretation of these parameters in terms of molecular structure, thus disallowing their use to monitor extent of enzymatic hydrolysis (Cruz, 1976).

The power law

$$\tau = K\gamma^N \qquad (2)$$

has successfully correlated shear stress-shear rate relationships for numerous materials including starch pastes (Farrow et al., 1928; Richardson and Waite, 1933; Higginbotham, 1947; Lancaster et al., 1966; Schutz and Nedonchelle, 1968). Its simplicity has encouraged its use, and attempts have been made to rationalize its form theoretically (Scott Blair, 1965, 1967). The sensitivity of K and N to changes in the consistency of a material (for example, starch pastes), could provide means to monitor the progress of an hydrolysis reaction.

This work examines the shear stress vs. shear rate behavior of enzyme free Amioca starch pastes (waxy maize) subsequent to varying degrees of hydrolysis by an immobilized α-amylase paddle catalyst (Cruz and Ollis, 1976). The resulting τ, γ measurements are interpreted by a power law relationship. A model for partially hydrolyzed starch is presented based on observed flow behavior.

In dilute polymer solutions, a useful parameter is the total hydrodynamic volume ϕ_e, which is the sum of the molecular polymer volume and the associated volume of immobilized solvent. Here, this parameter is shown to provide a convenient means of correlating viscosity vs. shear rate measurements at the higher polymer concentrations used in this study. The viscosity vs. volume fraction be-

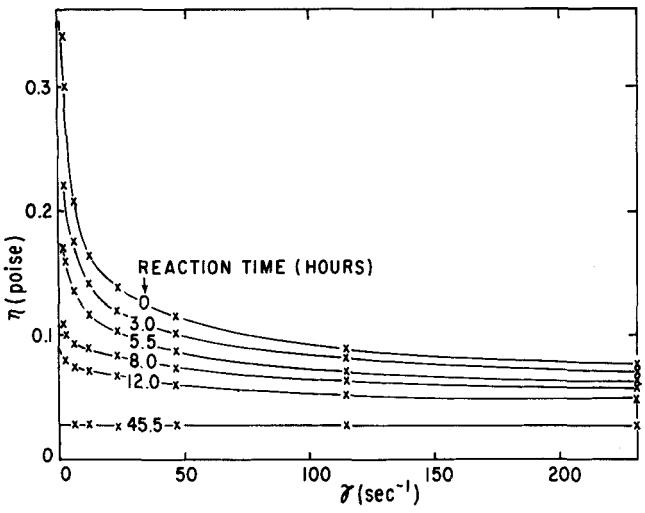

Fig. 1. Viscosity (η) vs. shear rate (γ) for (1.65% wt/vol) Amioca starch paste after varying hydrolysis times (hr) (rotating α-amylase paddle, 23°C).

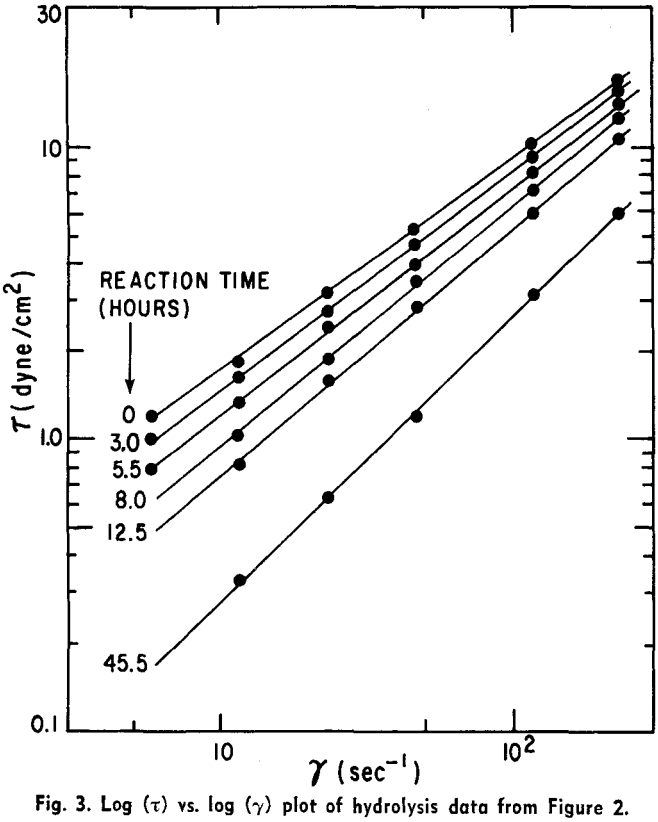

Fig. 3. Log (τ) vs. log (γ) plot of hydrolysis data from Figure 2.

havior of Amioca starch pastes and its hydrolysis products is compared to that of three other concentrated systems containing either rigid latex spheres, oil/water emulsions, or blood cells.

MATERIALS AND METHOD

Preparation of the nylon or steel mesh immobilized enzyme paddles used in this work is described elsewhere (Cruz and Ollis, 1976). Starch pastes were prepared by cooking a given amount of Amioca starch (waxy maize, >95% amylopectin, National Starch and Chemical Corp.) in *p*H 6.0, 0.04M acetate buffer for 2 to 3 hr at 100°C. Continuous agitation (turbine impeller, 240 rev/min) was needed to rupture the swollen granules. Solution concentrations were determined conveniently and reproducibly

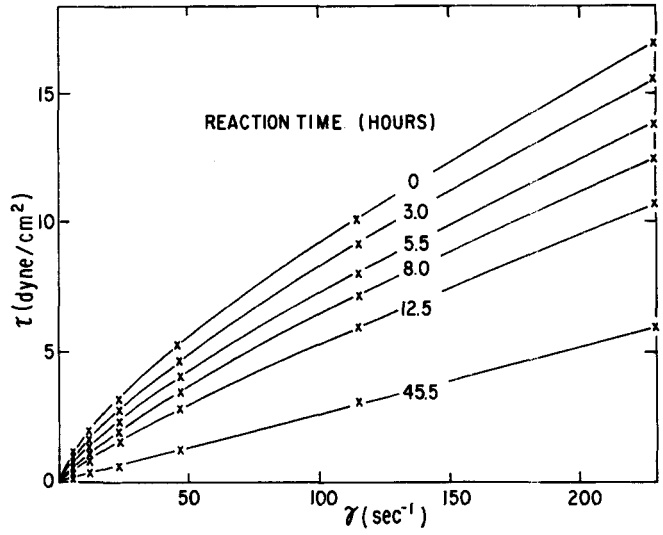

Fig. 2. Shear stress-shear rate data for the same samples as shown in Figure 1.

by drying samples to constant weight in a vacuum oven at 110°C over a bed of Celite (Sargent Welch).

In each batch experiment, an immobilized α-amylase paddle was immersed in 700 ml of starch paste contained in a glass beaker. Samples were taken periodically from the agitated reactor, diluted when necessary, and transferred to a Wells-Brookfield (model LVT) cone and plate viscometer. The viscometer cell temperature was controlled with a circulating constant temperature bath. In all cases, no enzyme hydrolysis occurred during the viscosity measurements; the absence of α-amylase leaching from the paddles is shown elsewhere (Cruz and Ollis, 1976).

RESULTS AND DISCUSSION

Degradation Flow Curves and the Power Law

The degree of hydrolysis of a starch paste can be followed by monitoring either reducing sugars, iodine staining ability (for high amylose containing starches), or viscosity. Of these possibilities, viscosity is the most sensitive to variations of starch molecular size. The observed viscosity behavior of starch pastes requires that a full flow curve be determined to fully characterize the material. Most starch pastes are thixotropic, thus exhibiting time-dependent viscosities; only those pastes composed predominantly of the branched component amylopectin provide time-independent viscosities (Storey and Merrill, 1958). Hence, the choice of Amioca starch for this study.

Figure 1 presents measured viscosity vs. shear rate for a 1.65% wt/vol Amioca paste previously hydrolyzed for the times indicated at 23°C with a rotating immobilized α-amylase mesh paddle. The curve at time = 0 illustrates characteristic shear thinning: the measured viscosity drops monotonically with increasing shear rates. The difficulty in applying a model, such as Equation (1), which requires at least one viscosity asymptote is apparent from Figure 2, since asymptotic behavior is not observed in the shear rate range attainable. As hydrolysis proceeds, the viscosity decreases over all shear rates.

The power law [Equation (2)] is an empirical relationship between shear stress (τ) and shear rate (γ) which is typically applied to that portion of material flow curves between the high and low shear asymptotes of zero- and infinite-shear viscosities, respectively.

The material constant N measures the departure from Newtonian ($N = 1.0$) behavior. The constant K is numerically equal to the viscosity coefficient at unit shear rate, but its dimensions depend on the value of N. For our pur-

poses, K will be identified as a unit shear viscosity, that is, $K = \eta_1$. The power law has been shown to adequately describe the behavior of aqueous starch pastes composed of amylose and amylopectin over a wide range of concentrations (Farrow et al., 1928; Richardson and Waite, 1933; Higginbotham, 1947; Lancaster et al., 1966; Schutz and Nedonchelle, 1968). For the same experiments shown in Figure 1, the nonlinear relation between shear stress and shear rate presented in Figure 2 illustrates the non-Newtonian behavior of all samples but one. At 45.5 hr of reaction time, the material appears to be Newtonian since $\eta \neq f(\gamma)$. When the data is plotted as (Figure 3)

$$\log \tau = \log \eta_1 + N \log \gamma \qquad (3)$$

a straight line adequately represents each data set, indicating the utility of the power law in the experimental range $5.75 \leq \gamma \leq 230\ s^{-1}$ for native and partially hydrolyzed Amioca starch pastes.

Table 1*a* summarizes the variations of N and η_1 with hydrolysis time. Unit shear viscosity decreases with time, while the index of non-Newtonian behavior N increases from 0.73 to 0.98 (essentially Newtonian) at 45.5 hr of reaction. Tables 1*b* and 1*c* represent the variations of η_1 and N with starch concentration and temperature of shear viscosity measurements, respectively. Unit shear viscosity increases rapidly with concentration. Samples with concentrations less than 0.63% wt/vol appear to be Newtonian; those with $c > 1\%$ wt/vol exhibit deviations from Newtonian behavior which are greater with increasing concentrations (Table 1*b*). The unit shear viscosity (η_1) decreases with increasing temperature, a result of decreasing solvent viscosity $\eta_o(T)$ as evidenced by a nearly constant relative viscosity, $\eta_r \equiv \eta_1/\eta_o$. This result suggests little or no expansion of the amylopectin molecules with temperature. The index of non-Newtonian behavior N is not a function of temperature (Table 1*c*) in agreement with Schutz and Nedonchelle's (1968) findings with 3% potato starch paste (≈80% amylopectin).

In two systems where consistency increases with time, a unique relationship between η_1 and N has been reported. Nedonchelle and Schutz (1967) followed retrogradation of starch pastes arising from hydrogen bonding between amylose molecules. At constant temperature they found

$$\log \eta_1 = \log \tau_o - N \log \gamma_o \qquad (4)$$

where τ_o and γ_o were constants. Later, Tuczyncki and Scott Blair (1967) observed the same behavior during coagulation of milk after addition of the enzyme rennet. In both systems, increases in viscosity with time were due to structure buildup among the elementary particles (molecules). Combination of Equations (3) and (4) gives

$$\log \tau = \log \tau_o - N \log \gamma_o + N \log \gamma$$

or

$$\frac{\tau}{\tau_o} = \left(\frac{\gamma}{\gamma_o}\right)^N \qquad (5)$$

Since N changes in time, τ_o and γ_o have dimensions of stress and shear rate, respectively. From Equation (5) when $\tau = \tau_o$, $\gamma = \gamma_o$. Thus, for each system satisfying Equation (4), a unique point (τ_o, γ_o) exists which is common to all τ-γ curves independent of N, the power law index. This was established experimentally for coagulating milk (Tuszynski and Scott Blair, 1967), where extrapolations of log τ vs. log γ plots all met at a common point (τ_o, γ_o).

As a starch paste undergoes hydrolysis, structure is destroyed in the sense opposite to the retrogradation or coagulation, the previous examples fitting Equation (4).

Table 1*a*, *b*, *c*. Variations of Power Law Parameters for Amioca Starch Paste

a. With degree of hydrolysis (1.65% wt/vol, 25°C)

Reaction time, hr	Unit shear rate viscosity $K \equiv \eta_1 \left[\frac{\text{dyne-(s)}^N}{\text{cm}^2}\right]$	Non-Newtonian index (N)
0.0	0.32	0.73
3.0	0.26	0.75
5.5	0.20	0.78
8.0	0.14	0.83
12.5	0.10	0.85
45.5	0.03	0.98

b. With concentration (no hydrolysis, 23°C)

Concentration, % wt/vol	Unit shear rate viscosity $K \equiv \eta_1 \left[\frac{\text{dyne-(s)}^N}{\text{cm}^2}\right]$	Non-Newtonian index (N)
3.14	3.40	0.61
2.51	1.70	0.62
2.20	1.20	0.65
1.88	0.71	0.66
1.57	0.38	0.71
1.26	0.17	0.78
0.63	0.03	0.94

c. With temperature (no hydrolysis, $c = 1.57\%$ wt/vol)

Temperature, °C	Unit shear rate viscosity $K \equiv \eta_1 \left[\frac{\text{dyne-(s)}^N}{\text{cm}^2}\right]$	Relative viscosity $\eta_r \equiv \eta_1/\eta_o$ $(s)^{N-1}$	Non-Newtonian index (N)
23.0	0.38	40.1	0.71
30.0	0.30	36.9	0.73
35.2	0.27	36.6	0.73
40.0	0.25	38.1	0.73
44.8	0.23	38.9	0.73
50.1	0.22	40.1	0.73
54.8	0.20	39.1	0.74
59.8	0.18	39.3	0.73

* η_o = viscosity of solvent at given temperature.

Values of η_1 and N obtained from Figure 3 were plotted in Figure 4 according to Equation (4). Clearly, the relationship holds indicating the existence of a point (τ_o, γ_o) = [369 (from intercept), 15 118 (from slope)] where all flow curves of Figure 3 meet upon extrapolation as confirmed in Figure 5.

Tuszynski and Scott Blair (1967) thought that such a point might represent the destruction by shear of all multiple particle structure, but their experiments indicated that this point was reached at a much lower rate of shear than γ_o and at shear rates which were not independent of the age of the coagulating milk sample.

For the flow curves of partially hydrolyzed Amioca starch paste, the ratio of τ_o to γ_o is $\eta^\infty \equiv \tau_o/\gamma_o$; it will be considered as the limiting viscosity at high shear rates. This ratio is $\eta^\infty = 369/15\,118 = 0.024$ poise (Figure 5); the significance of η^∞ will be discussed later.

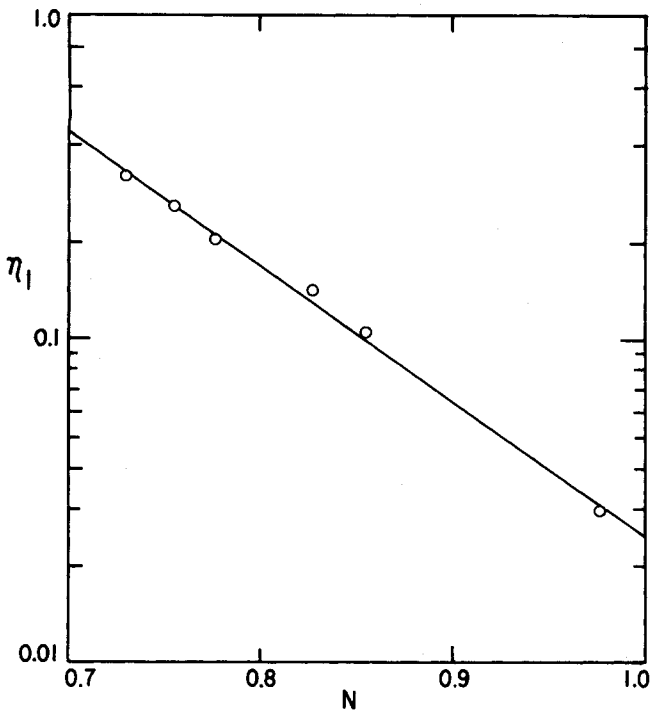

Fig. 4. Relationship between power law parameters from data in Figure 3.

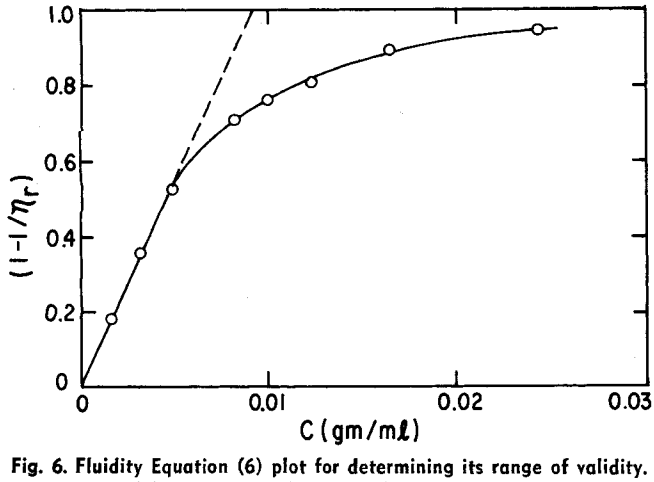

Fig. 6. Fluidity Equation (6) plot for determining its range of validity. (Slope of broken line = [η] = 110 ml/g.)

In the following section, shear dependent viscosities of 1.65 to 4.7% wt/vol Amioca starch pastes are correlated with ϕ_e, the total hydrodynamic volume of polymer plus associated liquid, as determined from dilute solution viscosity measurements.

Interpretation of ϕ_e at High Concentrations

We have shown elsewhere that Equation (6), the fluidity equation, can adequately predict intrinsic viscosities of Amioca starch solutions (Cruz and Ollis, 1976):

$$1 - 1/\eta_r = c[\eta] \qquad (6)$$

The total hydrodynamic volume (polymer plus immobilized liquid) per unit volume of solution ϕ_e was obtained for dilute solutions from the relationship (Cruz and Ollis, 1976)

$$\phi_e = \frac{c[\eta]}{2.5} \qquad (7)$$

Figure 6 establishes that linearity between $1 - 1/\eta_r$, and c holds for $(1 - 1/\eta_r) \leq 0.55$ (that is, $\phi_e \leq 0.22$) with Amioca starch paste. From Equation (7), the total

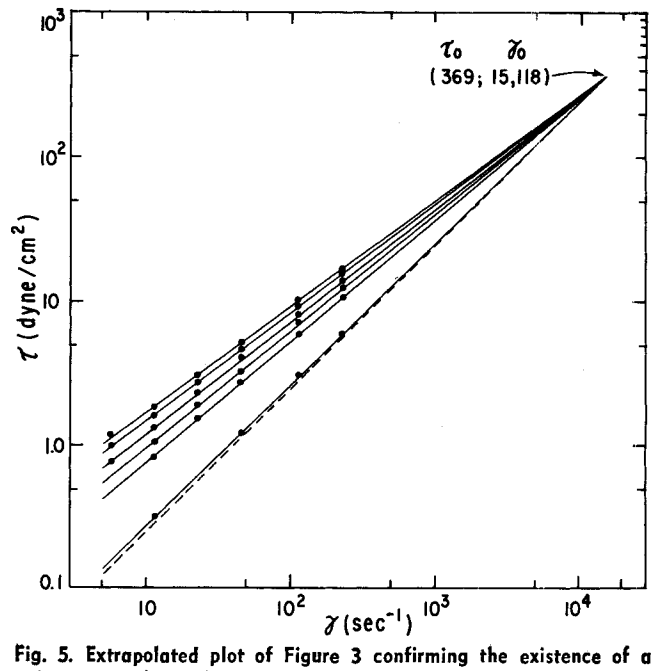

Fig. 5. Extrapolated plot of Figure 3 confirming the existence of a unique point (τ_o, γ_o) where all curves meet (broken line represents the Newtonian sample $\eta^\infty \equiv \tau_o/\gamma_o = 0.024$ poise).

volume fraction ϕ_e may be varied by changes of the concentration of polymer c or its molecular size as reflected in the intrinsic viscosity $[\eta]$. Once $[\eta]$ is obtained from diluted solutions ($c \lesssim 0.6\%$ wt/vol) using Equation (6), we may use Equation (7) to provide a correlation variable ϕ_e for viscosities of the original higher concentrations of starch in the sample solutions. This procedure allows use of a conveniently calculated variable ϕ_e for concentrated solutions without the need to account for compressibility effects. Dreval et al. (1973) and Simha and Utracki (1973) examined data for concentrated solutions of linear, flexible polymers. They have obtained single master curves for zero shear viscosity vs. reduced concentration plots where parameters similar to ϕ_e ($\equiv c[\eta]/2.5$) were used as the concentration variable: $Kmc[\eta]$ (Dreval et al., 1973), $c[\eta]$ (Dreval et al., 1973), or $c\zeta$ (Simha and Utracki, 1973). In these previous reports, Km = Martin's constant reflecting solvent effects, and ζ = molecular weight dependent parameter.

For each Amioca starch concentration, shear stress vs. shear rate plots were used to obtain values for the unit shear viscosity (η_1). For each value of η_1, ϕ_e is calculated by using Equations (6) and (7). Plotting ϕ_e vs. log $\eta_{r,1}$ [where the reduced viscosity in (seconds)$^{N-1}$, $\eta_{r,1} = \eta_1/\eta_o$] results in Figure 7 (broken line, two runs; +, *). Also shown are corresponding data of Maron et al (1951) and Maron and Madow (1953) similarly evaluated for synthetic nonswelling latexes [curve A (Maron et al. (1951)]: VGR-S, 80:20 butadiene-styrene copolymer emulsified with a mixture of Dresinate 731 and potassium oleate, avg. diam. = 1 920Å; curve B [Maron and Madow (1953]: aqueous dispersion of 50:50 butadiene styrene copolymer, potassium soap of K-wood rosin emulsifier, volume to surface avg. diam. = 800 to 1 100Å). Even though the viscosity of synthetic latexes varies with particle size, size distribution, and emulsifying agent, it appears that the $\eta_{r,1} - \phi_e$ relationship for starch paste coincides with the latex data (ϕ = latex volume fraction) for $\phi_e \lesssim 0.4$. This observation suggests that the unit shear rate behavior of Amioca starch paste approximates that of spherical incompressible latex particles at low volume fractions when ϕ_e for the starch is determined according to

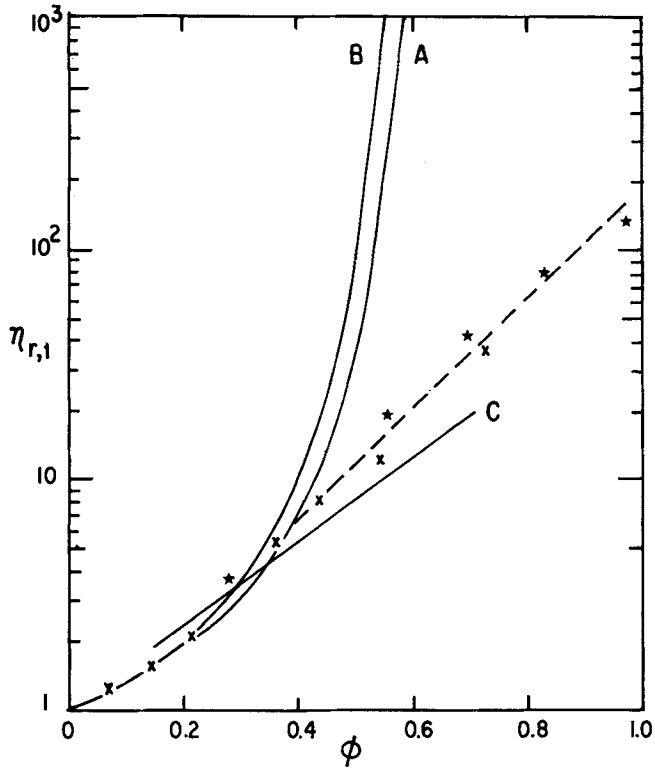

Fig. 7. Comparison of relative viscosity at unit shear rate ($\eta_{r,1}$) vs. volume fraction: Amioca starch paste, two experiments, (broken line; x, ⁎); synthetic spherical latexes (solid curves; A, B); human blood cells (solid curve C); $\phi = \phi_e$ for starch paste. See text for references.

Equation (7). For all higher volume fractions ϕ or ϕ_e, the latex's relative viscosities increase sharply, whereas the deformable and compressible starch structures exhibit a lower relative viscosity.

Linear log η_r vs. ϕ relationships such as observed with starch for $\phi_e \gtrsim 0.4$ (Figure 7) have been reported for suspensions of blood cells, emulsions of oil in water, benzene in water, and asphalt in oil (Richardson, 1953). Unit shear viscosity data available for heparinized dog blood, solid line C (Figure 7), represents this relationship (Gregersen et al., 1965). The linear form of the log η_r vs. ϕ_e data for large ϕ_e for deformable starch indicates that we can consider these concentrated pastes as being composed of deformable hypothetical particles which have dilute solution values of the ratio (polymer volume/immobilized liquid volume).

Viscosity-Volume Fraction (ϕ_e) Behavior of Partially Hydrolyzed Amioca Paste

Amylopectin molecules, which possess approximately 5% branch points [$\alpha - (1 \rightarrow 6)$ linkages], resemble a bushlike structure. Light scattering determinations of molecular weights and radius of gyration of amylopectin and its β-amylase limit dextrin by Stacy and Foster (1956) suggest that amylopectin molecules consist of a spherically symmetrical distribution of matter of continuously decreasing polysaccharide density with increasing radial position. Intrinsic viscosities reported in 1.0N potassium hydroxide were 127 for parent corn amylopectin and 122 for the β-amylase limit dextrin (Stacy and Foster, 1956). Similar results were obtained by Lansky et al. (1949) (121 for corn amylopectin, 125 for limit dextrin) and by Kerr et al. (1951) (145 and 117, respectively). These small decreases in intrinsic viscosities upon repeated removal of maltose (disaccharide) by β-amylase hydrolysis led Foster (1965) to conclude that most of the hydrodynamic effects of the amylopectin molecules are due to the branched structure in the molecule. Apparently, the

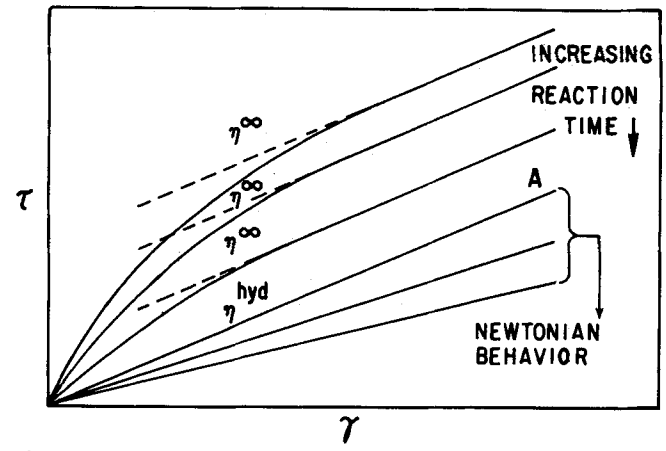

Fig. 8. Proposed shear stress-shear rate behavior of a Amioca starch paste undergoing immobilized enzyme hydrolysis. Curve A marks the onset of Newtonian behavior.

outer linear loose ends offer little resistance to solvent flow as supported by the lack of dependence of intrinsic viscosity upon shear rates in the range of 0.5 to 1 200 s^{-1} (Banks et al., 1972). This result indicates that ϕ_e determined from Equations (6) and (7) is dominated by the branched structures in the molecule. The α-amylase of the present study can hydrolyze even limit dextrins; this will give rise to a change of η due to a change of ϕ_e as we show later.

The non-Newtonian behavior exhibited by pastes of these native bushy structures has been attributed (Storey and Merrill, 1958) to association links between the outermost chain ends. With this interpretation and the light scattering data, we may formulate the following scenario for starch hydrolysis by α-amylase. Upon enzyme attack, the number of such outside accessible chains should be progressively diminished. If these extended chain ends are considered responsible for association links between molecules, their elimination through hydrolysis would result in decreased non-Newtonian behavior.

The percent change of viscosity as starch hydrolysis proceeds decreases with increasing shear rate (Figure 1); thus, after 12.5 hr of hydrolysis, there has been a 76.5% decrease at 23 s^{-1} as compared to a 36.5% at 230 s^{-1}. This result appears to indicate the importance of particle-particle association links on the low shear viscosity. High shear viscosities are only weakly affected by the presence of these link-forming chain ends. Continuing the above picture, after hydrolysis of the outermost chain ends, subsequent immobilized enzyme degradation of the remaining molecule slows down considerably. The remaining interior portion of the molecule possesses an effective hydrodynamic volume, here denoted as ϕ_e^{hyd}. If the high shear rate hydrodynamic volume contribution of the outermost free chain ends is considered to be negligible, then independent of degree of such chain hydrolysis, all hydrolysis samples should exhibit the same high shear rate hydrodynamic volume (ϕ_e^∞) and therefore infinite shear viscosity (η^∞) (prior to subsequent slow hydrolysis of the remaining interior).

Such a conclusion is consistent with our finding that all log τ — log γ curves of a hydrolyzing paste extrapolate to one common high shear point (Figure 5). From the previous remarks, this common point may be considered to represent a viscosity (η^∞) influenced only by the total effective hydrodynamic volume of suspended particles at high shear rates (ϕ_e^∞). For the above statements to be correct, the τ vs. γ plots for an hydrolysis reaction as depicted in Figure 8 must all have the same slope η^∞ (broken lines) at high shear rates which must correspond

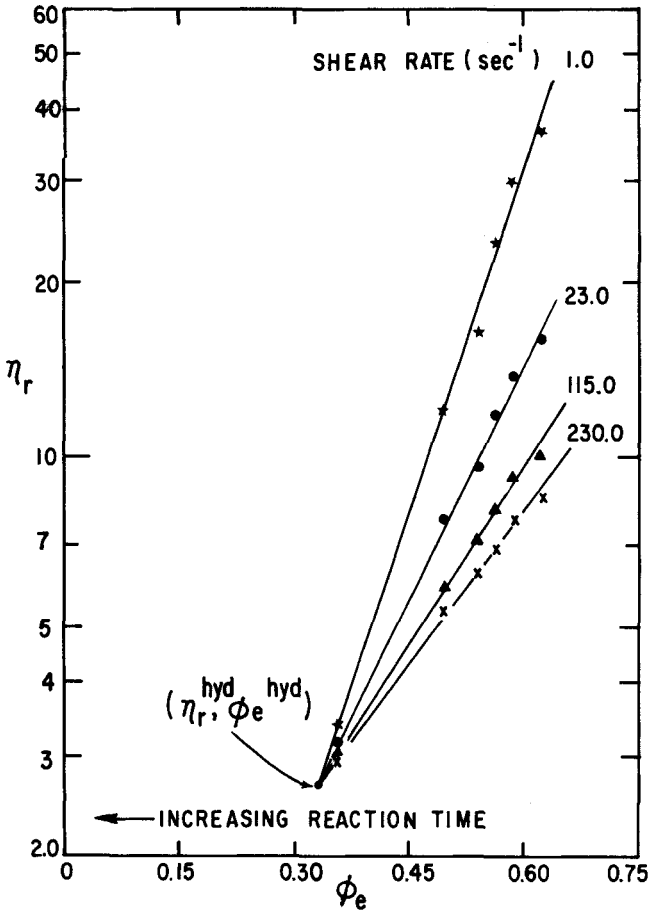

Fig. 9. Plot of log η_r vs. ϕ_e at varying shear rates. The common intersection (η_r^{hyd}, ϕ_e^{hyd}) permits the determination of the first appearance of Newtonian behavior.

to the viscosity (η^{hyd}) of the hydrolyzed material first exhibiting Newtonian behavior (curve A). The experimental τ vs. γ data presented in Figure 2 do not include sufficiently large shear rates to verify this argument, since we would need $\gamma > 15\,118\ s^{-1}$ as seen from Figure 5. Nevertheless, the extrapolated point obtained from the log τ vs. log γ point of these data ($\eta^{\infty} = 0.024$ poise, Figure 5) agrees well with the slope (Figure 2, time = 45.5 hr, slope = $\eta = \tau/\gamma = 0.026$ poise) of the sample which is approaching Newtonian behavior ($N = 0.98$, Table 1*a*).

Analysis of the τ vs. γ hydrolysis data and experimental evaluation of ϕ_e allowed determination of the viscosity η_r^{hyd} and volume fraction (ϕ_e^{hyd}) at the onset of Newtonian behavior. In Figure 7, increases in ϕ_e were brought about by increasing the concentration and by maintaining [η] constant (that is, no hydrolysis). When a starch paste undergoes enzymatic hydrolysis, the total saccharide concentration is maintained constant, while hydrolysis results in decreasing values for [η], hence of ϕ_e.

To obtain the limiting point (η_r^{hyd}, ϕ_e^{hyd}), the relative viscosity (η_r) may be plotted against the total equivalent hydrodynamic volume (ϕ_e), with shear rate as the third parameter. As mentioned previously, Amioca starch pastes exhibit flow behavior similar to that observed for deformable bodies [for example, blood cell suspensions and oil/water and benzene/water emulsions, Richardson, 1953], that is, linear log η_r vs. ϕ_e plots. This is shown to be true for a range of shear rates in Figure 9, where the data from Figure 2 (as log η_r) follow a linear relationship to ϕ_e. It is not possible to determine directly the volume fraction of polymer molecules plus immobilized liquid in concentrated solutions. Values for ϕ_e were obtained by a

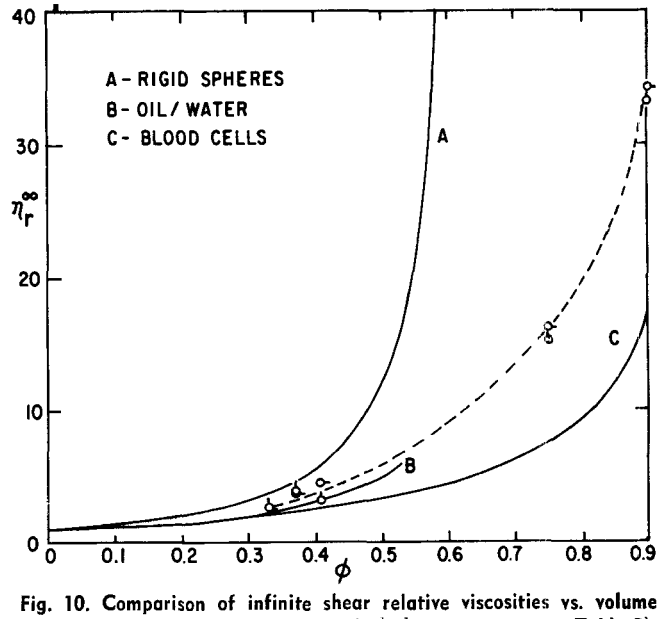

Fig. 10. Comparison of infinite shear relative viscosities vs. volume fraction data: Amioca starch pastes (η_r^{hyd}—o–; η_r^{∞}—o—; Table 2); butadiene-styrene latex rigid spheres (A); oil-water emulsions (B); and blood cells (C); $\phi = \phi_e^{hyd}$ for starch paste. See text for references.

Table 2. Tabulation of Extrapolated Limiting Viscosities and Volume Fractions

Run No.	Conc., % wt/vol	Paddle type*	From log τ vs. log γ plots η_r^{∞}	From log (η_r) vs. ϕ_e plots η_r^{hyd}	From log (η_r) vs. ϕ_e plots ϕ_e^{hyd}
1	1.65	ROT	2.74	2.65	0.33
2	1.70	REC 1	4.49	3.18	0.41
3	2.17	REC 2	3.75	3.80	0.37
4	3.03	REC 1	16.2	15.2	0.75
5	4.68	REC 1	34.2	33.2	0.90

* ROT = rotating paddle; REC = reciprocating paddles.

threefold dilution of the sample (that is, from 0.0165 to 0.0055 g/ml), determining ϕ_e' of the diluted sample with the use of Equation (6), and then using $\phi_e = 3\phi_e'$.

If the data of Figure 9 are extrapolated, all lines meet at the same point (η_r^{hyd}, ϕ_e^{hyd}). From these coordinates, the viscosity ($\eta_r^{hyd} \equiv \eta^{hyd}/\eta_o = 2.65$) and the equivalent volume fraction at which Newtonian behavior is first observed, $\phi_e^{hyd} = 0.33$) may be determined. Table 2 summarizes the results for five runs, each corresponding to different initial starch concentration and the amylase paddles indicated. These results are derived by data reduction according to Figures 4, 5, and 9. Values for η_r^{∞} from log τ vs. log γ plots are compared with η_r^{hyd} values obtained from graphs of log η_r vs. ϕ_e (from example, Figure 9). Good agreement is observed. The corresponding ϕ_e^{hyd} values are also tabulated.

Our experimental data show that $\eta_r^{\infty} \approx \eta_r^{hyd}$. If we assume the same functional relationship between viscosity (η_r) and total effective hydrodynamic volume (ϕ_e) for η_r^{∞} and η_r^{hyd}, it follows that ϕ_e^{∞} must equal ϕ_e^{hyd}. Presently, we do not know if this result is general or if it only describes the system at hand. As determination of ϕ_e^{∞} is impossible through direct experimentation, the above reasoning provides a relationship between the shear limiting viscosity (η_r^{∞}) and volume fraction (ϕ_e^{∞}) when we take $\phi_e^{\infty} = \phi_e^{hyd}$.

It is of interest to compare the values for η_r^{hyd} and ϕ_e^{hyd} with existing infinite shear viscosities—volume fraction

data for systems of rigid spheres and deformable bodies. Figure 10 presents such a comparison (o for η_r^{hyd} from log η_r vs. ϕ_e; o- for η_r^{∞} from log τ vs. log γ). Hydrolyzed Amioca starch particles exhibited an average radius of gyration in the order of ~1 200Å when taken as polydisperse random coils or 533Å when assumed to be monodisperse spheres (Cruz and Ollis, 1976). A butadiene-styrene latex (Maron and Folk, 1955) with average particle diameter = 1 390Å represents the $\eta_r^{\infty} - \phi$ relationship for rigid spheres. The oil/water emulsion data (polydispersed oil drop size distribution of approximately 65% within the 0.5 to 2.0μ diameter range) from Parkinson et al. (1970) at high shear rates (1 468 s^{-1}) and Bayliss's (1952) apparent asymptotic viscosity (η_r) for dog's blood (corpuscles are approximately 5 to 10μ in diameter and 1.5 to 2.5μ thick) represent two examples of high shear rate deformable body behavior.

From Figure 10, the limiting shear viscosity of an Amioca starch paste $\eta_r^{\infty} \approx \eta_r^{hyd}$ follows a volume fraction-viscosity behavior (broken line; δ, o-) which falls between that of rigid spheres and easily deformable bodies. This physically reasonable behavior obtains when the volume fraction is taken to be the residual hydrodynamic volume fraction ($\phi_e^{hyd} = \phi_e^{\infty}$) resulting from Figure 9. This behavior substantiates the proposed view of the ratio (τ_o/γ_o) as an infinite shear viscosity η^{∞}.

Our observation for Amioca paste (branched amylopectin molecules) of a unique relationship between η_r and ϕ_e (Figures 9, 10, and 11) parallels the earlier finding for linear flexible molecules of a dimensionless concentration reducing variable (Dreval et al., 1973; Simha and Utracki, 1973). In addition, we have been able to assign a physical interpretation to ϕ_e and have shown that the $\eta_r - \phi_e$ relationship holds for all shear rates in our study range (3.0 to 230 s^{-1}, Figure 9), as well as for the extrapolated limiting shear viscosity η_r^{∞} ($= \eta_r^{hyd}$) (Figure 10).

ACKNOWLEDGMENT

We are grateful to the government of Puerto Rico for a research fellowship for Angel Cruz. The support of the Eppley and National Science Foundation is appreciated.

NOTATION

a = radius of particle
c = concentration
C_1, C_2, C_3, n = material constants in Equation (1)
k = Boltzmann's constant
K = power law constant $\equiv \eta_1$
Km = Martin's constant
N = power law index of non-Newtonian behavior
T = temperature

Greek Letters

γ = shear rate
γ_o = characteristic shear rate
ζ = molecular weight dependent parameter
η = viscosity of suspension
η_1 = viscosity at unit shear rate [$\equiv$ power law constant (K)]
η_o = solvent viscosity
η_r = relative viscosity ($\equiv \eta/\eta_o$)
$\eta_{r,1}$ = unit shear rate relative viscosity ($\equiv \eta_1/\eta_o$)
η^{hyd} = viscosity of hydrolyzed material first exhibiting Newtonian behavior
η_r^{hyd} = relative viscosity of hydrolyzed material first exhibiting Newtonian behavior ($\equiv \eta^{hyd}/\eta_o$)
η^{∞} = shear limiting Newtonian viscosity
η_r^{∞} = shear limiting relative viscosity ($\equiv \eta^{\infty}/\eta_o$)
$[\eta]$ = intrinsic viscosity
τ = shear stress
τ_o = characteristic shear stress
τ_r = reduced shear stress
ϕ = volume fraction
ϕ_e = total hydrodynamic volume of polymer plus immobilized liquid
ϕ_e' = total hydrodynamic volume of polymer plus immobilized liquid of diluted sample
ϕ_e^{∞} = limiting shear total hydrodynamic volume of polymer plus immobilized liquid
ϕ_e^{hyd} = total hydrodynamic volume of hydrolyzed molecules plus immobilized liquid for sample first exhibiting Newtonian behavior

LITERATURE CITED

Banks, W., R. Geddes, C. T. Greenwood, and I. E. Jones, "Physicochemical Studies on Starches," *Die Stärke*, **24**, No. 8, 245 (1972).

Bayliss, L. E., "Rheology of Blood and Lymph," in *Deformation and Flow in Biological Systems*, A. Frey Wyssling, ed., p. 362, North-Holland, Amsterdam (1952).

Cross, M. M., "Polymer Rheology: Influence of Molecular Weight and Polydispersity," *J. App. Polymer Sci.*, **13**, 765 (1969).

Cruz, Angel, "Kinetics and Shear Viscosity Characterization of Starch Hydrolysis with Immobilized α-Amylase," Ph.D. thesis, Princeton Univ., Princeton, N. J. (1976).

———, and D. F. Ollis, "Immobilized Amylase Hydrolysis of High Molecular Weight Starch Solutions," submitted to *Biotechnol. Bioeng.* (1976).

Dreval, V. E., A. Y. Malkin, and G. O. Botvinnik, "Approach to Generalization of Concentration Dependence of Zero-Shear Viscosity in Polymer Solutions," *J. Polymer Sci., Polymer Physics*, **11**, 1055 (1973).

Farrow, F. D., G. M. Lowe, and S. M. Neale, "II. The Flow of Starch Pastes—Flow at High and Low Rates of Shear," *J. Textile Inst.* **19**, No. T18-31 (1928).

Foster, J. F., "Physical Properties of Amylose and Amylopectin in Solution," in *Starch: Chemistry and Technology*, R. L. Whistler and E. F. Paschall, ed., Academic Press, Vol. 1, p. 349, New York (1965).

Gillespie, T., "Analysis of the Flow of Shear Thinning Colloidal and Polymeric Systems Which Exhibit Elastic Recovery or Rigidity," *J. Colloid Interface Sci.*, **22**, 563 (1966).

Gregersen, M. I., B. Peric, S. Chien, D. Sinclair, C. Chang, and H. Taylor, "Viscosity of Blood at Low Shear Rates: Observations on Its Relation to Volume Concentration and Size of the Red Cells," in *Proceedings 4th International Congress on Rheology Part 4*, Interscience, New York, Alfred L. Copley, ed., p. 613 (1965).

Higginbotham, R. S., "The Flow of Starch Pastes, Part IV. A New Consistometer for Starch Pastes and Some Results Obtained with It," *J. Textile Inst.*, **38**, T131 (1947).

Kerr, R. W., F. C. Cleveland, and W. J. Katzbeck, "The Molecular Magnitude of Amylopectin," *J. Am. Chem. Soc.*, **73**, 111 (1951).

Lancaster, E. B., H. F. Conway, and F. Schwab, "Power-Law Rheology of Alkaline Starch Pastes," *Cereal Chem.*, **43**, 637 (1966).

Lansky, S., M. Kooi, and J. Schoch, "Properties of the Fractions and Linear Substractions from Various Starches," *J. Am. Chem. Soc.*, **71**, 4066 (1949).

Maron, S. H., B. P. Madow, and I. M. Krieger, "Rheology of Synthetic Latex. II. Concentration Dependence of Flow in Type V GR-S Latex," *J. Colloid Sci.*, **6**, 584 (1951).

Maron, S. H., and B. P. Madow, "Rheology of Synthetic Latex. III. Concentration Dependence of Flow in Type III GR-S Latex," *ibid.*, **8**, 130 (1953).

Maron, S. H., and S. M. Fok, "Rheology of Synthetic Latex. V. Flow Behavior of Low Temperature GR-S Latex," *ibid.*, **10**, 482 (1955).

Nedonchelle, Y., and R. A. Schutz, "De l'homogénéité dimensionnelle de l'équation $\tau = kD^a$ caractérisant le comportement rhéologique des systémes aqueux de carbohydrates macromoléculaires," *Compt. Rend.*, **265**, C-16 (1967).

Parkinson, C., S. Matsumoto, and S. Sherman, "The Influence of Particle Size Distribution on the Apparent Viscosity of Non-Newtonian Dispersed Systems," *J. Colloid Interface Sci.*, **33**, No. 1, 150 (1970).

Powell, E. L., "Starch Amylopectin: (Waxy Corn and Waxy Sorghum)" in *Industrial Gums*, 2 ed., Chapt. 15, Academic Press, New York (1973).

Richardson, E. G., "Emulsions," in *Flow Properties of Dispersed Systems*, J. J. Hermans, ed., p. 53, North-Holland, Amsterdam (1953).

Richardson, W. A., and R. J. Waite, "The Flow of Starch Pastes. iii. The Effect of Soaps and Other Electrolytes on the Apparent Viscosity of Hot Starch Pastes," *J. Textile Inst.*, **24**, T383-416 (1933).

Schutz, R. A., and Y. Nedonchelle, "The Rheology of Concentrated Aqueous Carbohydrate Systems," in *Proceedings Annual 1966 Conference British Society Rheology*, R. E. Welton and R. W. Wharlow, ed., Macmillan, England (1968).

Scott Blair, G. W., "On the Use of Power Equations to Relate Shear-Rate to Stress in Non-Newtonian Liquids," *Rheol. Acta*, 4, 53 (1965).

———, "A Model to Describe the Flow Curves of Concentrated Suspensions of Spherical Particles," *ibid.*, **6**, 201 (1967).

Simha, R., and L. A. Utracki, "The Viscosity of Concentrated Polymer Solutions: Corresponding States Principles," *ibid.*, **12**, 455 (1973).

Stacy, C. J., and J. F. Foster, "A Light Scattering Study of Corn Amylopectin and Its Beta-Amylase Limit Dextrin," *J. Polymer Sci.*, **20**, 57 (1956).

Storey, B. T., and E. W. Merrill, "The Rheology of Aqueous Solutions of Amylose and Amylopectin with Reference to Molecular Configuration and Intermolecular Association," *ibid.*, **33**, 261 (1958).

Tuszyński, W., and G. W. Scott Blair, "Dimensionless Form of the Double Logarithmic Equation Relating Shear Stress to Shear Rate as applied to Slowly Coagulating Milk," *Nature*, **216**, 367 (1967).

Williams, J. M., "The Chemical Evidence for the Structure of Starch," in *Starch and its Derivatives*, J. A. Radley, ed., 4 ed., p. 91, Chapman and Hall, England (1968).

Manuscript received April 1, 1976; revision received May 25, and accepted May 27, 1976.

Dynamics of Aerosol Coagulation and Condensation

The dynamic behavior of aerosol size distributions under the influence of coagulation and growth by heterogeneous condensation of gaseous species is studied. Analytical solutions are obtained to the integro-differential equation governing the aerosol size distribution density function. Two modes of coagulation (constant and linear coagulation constants) and two modes of condensation (growth independent of particle volume and linearly dependent on particle volume) are considered. The interaction of the two growth mechanisms on aerosol size distributions is elucidated.

T. E. RAMABHADRAN
T. W. PETERSON
and
J. H. SEINFELD

Department of Chemical Engineering
California Institute of Technology
Pasadena, California 91125

SCOPE

The growth of aerosols results from a variety of physical and chemical phenomena. For atmospheric aerosols, the most important phenomena are coagulation and heterogeneous condensation. Because of the strong dependence of aerosol properties, such as light scattering, on particle size, it is desirable to understand in as much detail as possible how a size distribution evolves under the influence of these two processes. The size distribution of an aerosol is described by its size distribution density function, which is governed in general by a partial integro-differential equation. For simulations of atmospheric aerosol dynamics including turbulent transport and dispersion, numerical solution of the equation will ultimately be necessary. However, analytical solutions for certain limiting cases of a spatially homogeneous aerosol can be valuable in understanding the qualitative structure of the behavior in more complex situations. The object of this work, therefore, is to obtain analytical solutions to the general equation governing the size distribution density function of an aerosol undergoing simultaneous coagulation and condensation. Beyond their utility in understanding atmospheric aerosol dynamics, the solutions should be helpful in describing the dynamic behavior of any particulate system in which coagulation and condensation are taking place.

CONCLUSIONS AND SIGNIFICANCE

Analytical solutions are obtained to the general dynamic equation governing the size distribution density function of an aerosol undergoing simultaneous growth by coagulation and heterogeneous condensation. The solutions elucidate the influences of simultaneous coagulation and condensation on the evolving size distribution of an aerosol. Because of the complexity of actual coagulation and condensation kinetics, it is necessary to assume simple functional forms for these processes to enable analytical investigation of the dynamics. Consequently, coagulation constants, independent of particle volume and dependent on the sum of the particle volumes, and condensation rates, independent of particle volume and linearly dependent on particle volume, are considered. A